On the $P\,2_1/m$ and *Pmmn* pathways of the B1–B2 phase transition in NaCl: a quantum-mechanical study

2004 J. Phys.: Condens. Matter 16 3909

(http://iopscience.iop.org/0953-8984/16/23/011)

INSTITUTE OF PHYSICS PUBLISHING JOURNAL OF PHYSICS: CONDENSED MATTER

J. Phys.: Condens. Matter **16** (2004) 3909–3921 PII: S0953-8984(04)77496-2

On the $P2_1/m$ and $Pmmn$ pathways of the B1–B2 phase transition in NaCl: a quantum-mechanical study

Michele Catti

Dipartimento di Scienza dei Materiali, Università di Milano Bicocca, via Cozzi 53, 20125 Milano, Italy

Received 3 March 2004
Published 28 May 2004
Online at stacks.iop.org/JPhysCM/16/3909
DOI: 10.1088/0953-8984/16/23/011

Abstract

The monoclinic $P2_1/m$ and orthorhombic $Pmmn$ (Watanabe *et al*'s-type) mechanisms of the high-pressure phase transition of NaCl between the B1 (rocksalt, $Fm\bar{3}m$) and B2 (CsCl-like, $Pm\bar{3}m$) cubic phases were investigated by *ab initio* DFT techniques with all-electron localized basis sets. Enthalpy profiles versus the order parameter were computed at constant pressures of 15, 26.3 (equilibrium) and 35 GPa for each pathway. The monoclinic path shows a lower activation enthalpy at the equilibrium pressure, but at different p values (hysteresis effects) the other mechanism becomes competitive. In the $P2_1/m$ case, sharp jumps of structural parameters are observed along the transformation coordinate, which can be explained by a mechanism based on discontinuous sliding of alternating pairs of (100) atomic layers. This accounts also for the predicted formation of a metastable intermediate $Cmcm$ phase with TlI-like structure, similar to that observed experimentally at high pressure in AgCl, and the relations with the KOH structure are discussed, too. On the other hand, along the $Pmmn$ pathway the structural parameters vary quite smoothly, indicating a continuous motion of neighbouring atomic planes within the constraint of the additional mirror symmetry.

(Some figures in this article are in colour only in the electronic version)

1. Introduction

The theory of phase transitions has been a fascinating field of solid state science for a long time, producing in particular quite successful achievements by means of phenomenological approaches like that by Landau and others. Following that route, the role of structural symmetry was investigated rigorously by group-theoretical techniques, so as to attain a

sophisticated capability of prediction of the qualitative thermodynamic features of solid–solid phase transformations [1]. This approach, though initially developed particularly for continuous or semi-continuous (both displacive and order–disorder) transitions, was also recently extended with success to discontinuous (reconstructive) transformations [2]. In that case there is no symmetry group–subgroup relation between the two phases involved in the transition, as in continuous transformations, but rather an intermediate structural state can be conceived, whose symmetry is a subgroup of the symmetry groups of both end phases. However, a purely phenomenological approach is not able to produce really quantitative predictions, as it does not take into account the quantum-mechanical nature of microscopic atom–atom interactions, which indeed rule the phase transition. Therefore, it is necessary to complement Landau-like approaches with first-principles calculations of the free energy landscape in the space of order parameters, so as to determine the least-energy pathways within the symmetry constraint predicted by the phenomenological theory. In this way, two goals can be attained: (i) to discriminate between different atomistic mechanisms, which are equally acceptable on symmetry grounds; (ii) to provide theoretical estimates of the thermodynamic and kinetic parameters of the transformation. In this respect, phase transitions driven by pressure are simpler to be dealt with, because static calculations at the athermal limit can be used on replacing the Gibbs free energy by the enthalpy $H = E + pV$, where E is the ground-state quantum-mechanical total energy.

In the frame of a research project on the theoretical mechanisms of reconstructive, first-order phase transformations induced by pressure, after considering the B3–B1 transition in SiC and ZnS [3, 4] we have begun an investigation of the B1 (NaCl-like structure, space group $Fm\bar{3}m$)–B2 (CsCl-like, $Pm\bar{3}m$) process. Several binary compounds with B1 structure transform into the denser B2 phase at higher pressure and/or at lower temperature. We shall summarize here the cases of alkali halides, silver halides, and alkaline-earth oxides. The thermodynamic phenomenology is known: at room temperature, only the B1 phase is observed for Li halides, only the B2 one for Cs halides other than CsF, which, together with all the Rb and K halides, transforms from B1 to B2 at pressures not higher than 5 GPa [5]. The case of Na halides is more complex: the B1–B2 transition pressure p_t is 27 GPa for NaF [6] and around 29–30 GPa for NaCl [7, 8], but NaBr and NaI transform from B1 to a TlI-type structure (orthorhombic $Cmcm$) in the 35–40 and 27–31 GPa ranges, respectively [6, 9]; a further transition to B2, though not observed below 50 GPa, should probably occur at higher pressure. AgCl undergoes a transition from B1 to a KOH-type (monoclinic $P2_1/m$) phase, then to the TlI-type structure and finally to B2 at $p_t = 7$, 11 and 17 GPa [10, 11]. AgBr and AgI transform to the KOH-type phase at 8 and 11 GPa, respectively [11]; the final transition to B2 is expected to occur at higher pressure [12]. As for alkaline-earth oxides, the B1–B2 transformation is reported to occur at $p_t = 60$, 36 and 9 GPa for CaO, SrO and BaO, respectively [13–15]. A number of quantum-mechanical studies have attempted to predict the phase stability ranges of the B1 and B2 structures in some of these compounds, employing different Hamiltonians and basis sets, and usually attaining a reasonable agreement with the experimental B1–B2 transition pressures [12, 16–19].

Much less experimental and theoretical work has been done on the kinetic and mechanistic aspect of the transformation. On crystal-chemical grounds, Buerger proposed a simple mechanism based on compression of the primitive cell of the B1 structure along its threefold axis, so as to increase progressively the rhombohedral angle of the intermediate $R\bar{3}m$ state from 60° to 90° and to attain the cubic B2 cell [20]. The problem was also studied experimentally, by analysing the relative crystallographic orientations of CsCl samples across the temperature-driven B2–B1 transition at 719 K [21]; the outcome suggested a different mechanism, based on shifts of adjacent (001) planes of B1 leading to an intermediate orthorhombic $Pmmn$ symmetry

(Watanabe's mechanism). Results of similar investigations on the pressure-driven transitions of RbI [22] and RbCl [23] are less easy to rationalize, but should incline more to the Buerger's model. On the theoretical side, we are aware of two studies concerning Buerger's [17] and Watanabe's [18] mechanisms, and of a full group-theoretical analysis of the symmetries of possible intermediate states of the B1–B2 reconstructive transformation [24]. Starting from the results of the latter paper, which suggested a mechanism based on a monoclinic $P2_1/m$ intermediate symmetry, we did a preliminary investigation of this pathway in the case of the B1–B2 transition of CaO [25]. As the most interesting finding, a metastable phase, corresponding to the orthorhombic $Cmcm$ TlI-type structure, was detected to be present along the monoclinic transformation path.

In this work, a detailed *ab initio* study of the monoclinic $P2_1/m$ and orthorhombic $Pmmn$ mechanisms of the B1–B2 transition of NaCl is presented. The DFT (density functional theory)–GGA (generalized gradient approximation) approach is used, with an all-electron basis set of Gaussian-like atomic orbitals, in order to compute the enthalpy profile at constant pressure versus the transformation order parameter. A full relaxation of all symmetry-unconstrained structural variables is included. In particular, we want to explore the effect of p values different from the equilibrium pressure p_t on the relative activation enthalpies of the two intermediate states, and on the stability of the intermediate TlI-type phase. Further, the relations of the monoclinic pathway with the KOH-type structure observed as a stable phase in the sequence of high-pressure transformations of other systems will be examined.

2. Computational method

All quantum-mechanical calculations were carried out by the computer code CRYSTAL03 [26], implementing a periodic LCAO (linear combination of atomic orbitals) approach in which the self-consistent-field equations for one-electron eigenvalues and crystalline orbitals can be solved by use of the Hartree–Fock or the DFT Hamiltonian, or even of mixtures of them. Here the DFT–GGA–PBE Hamiltonian [27] was employed, with all-electron localized basis sets based on 13 (Na) and 17 (Cl) atomic orbitals. The radial factors are expressed as linear combinations of Gaussian-type functions of the electron–nucleus distance, according to 8(s)511(sp)G and 8(s)6311(sp)G contractions for sodium and chlorine, respectively. The Gaussian parameters were taken from [28], but the exponents of the outer sp and d-type Gaussian functions were re-optimized by minimizing the total energy at the experimental room-pressure structural configuration. The level of numerical approximation in evaluating the Coulomb and exchange series appearing in the SCF equations for periodic systems is controlled by five tolerances [26]. These are related to estimates of overlap or penetration for integrals of Gaussian functions on different centres, which define cut-off limits for series summation. The values used in the present calculations are 10^{-8}, 10^{-8}, 10^{-8}, 10^{-8}, and 10^{-16}. The reciprocal space was sampled according to a regular sublattice defined by eight points in the Monkhorst grid (125 and 170 points in the irreducible Brillouin zones of the monoclinic and orthorhombic intermediate states of NaCl, respectively). Convergence was checked with respect both to tolerances and to the number of Monkhorst points, and it was controlled by a threshold ($\Delta E = 10^{-8}$ Hartree/ primitive unit cell) in the self-consistent-field cycles. In order to accelerate the SCF convergence, the technique of level shifter was used: that enhances the energy difference between highest occupied and lowest empty states in the first cycles.

Atomic coordinates were optimized by calculation of analytical gradients and subsequent conjugate gradients algorithm (OPTCOORD option). The unit-cell optimizations were performed by the LoptCG routine written by Zicovich-Wilson, which is based on computation of numerical derivatives of the total energy with respect to unit-cell constants, and subsequent

processing by conjugate gradients. The routine was modified so as to minimize the enthalpy H at a given pressure, rather than the energy at zero pressure as in the ordinary case. The technique of classifying the mono- and bi-electronic integrals according to a reference structure (FIXINDEX option of the code) was employed, in order to reduce the numerical noise of enthalpy curves calculated for structures with different volumes. A reference volume of 24.33 Å^3/NaCl formula unit, much smaller than those of all the structures considered, was used in all cases; the actual reference structures were obtained by rescaling their unit-cells so as to reduce the volume accordingly.

3. The transformation pathways

In a reconstructive phase transition, the intermediate structural state (IS) has a symmetry which is a subgroup of the space groups of both end phases; the latter, on the other hand, are quite unrelated to each other. Therefore the order parameter, or reaction coordinate (in the language of chemical kinetics) of the process, ξ, is a normalized structural degree of freedom of the IS which triggers an increase of symmetry when it takes its end values 0 (starting phase) or 1 (end phase). The choice of the order parameter among the degrees of freedom of the IS may not be unique; the other symmetry-unconstrained structural variables (lattice constants and/or atomic fractional coordinates) have to be relaxed, at constant pressure, so as to minimize the enthalpy of the IS for each value of ξ considered. In this way, enthalpy profiles $\Delta H(\xi, p)$ can be calculated for different pressure values, where the enthalpy of the IS is referred to that of the initial phase ($\xi = 0$).

In general, two types of reconstructive transformation mechanisms can be conceived [25]. In type I, atoms occupy the same sites before and after the transition, although the site symmetries are expected to change. A pure lattice distortion then characterizes the transformation, and should be taken as its order parameter. The fractional atomic coordinates in the low-symmetry reference frame are the same for both end phases; however, they usually change according to relaxation in the intermediate states. On the other hand, in type II a net atomic motion occurs along the transformation, so that the fractional coordinates of some atoms are different in the two end phases, and they build up the natural order parameter of the process; a lattice distortion may occur as an accessory phenomenon. The $R\bar{3}m$ (Buerger's) and $P2_1/m$ pathways of the B1/B2 transition belong to type I, whereas the $Pmmn$ (Watanabe's) one is of type II. Indeed, the $P2_1/m$ mechanism can be represented as a variant of the $R\bar{3}m$ one, as now the primitive unit-cell of the B1 structure is compressed along the long diagonal of one of its faces, rather than along the long diagonal of the cell itself, so that a monoclinic rather than rhombohedral intermediate symmetry is attained. In the $R\bar{3}m$ case the choice of the order parameter is unique (rhombohedral α angle), and no atomic relaxation is allowed by symmetry, whereas in the $P2_1/m$ intermediate state the x and z atomic coordinates can undergo substantial changes, and the order parameter is conveniently but not necessarily chosen to be the monoclinic β angle (cell-edge ratios could work as well). On the other hand, the $Pmmn$ pathway is driven by a net atomic motion along the [001] orthorhombic direction, so that the z coordinate of one of the two atoms (say, Na in the NaCl case) should be taken as the order parameter, leaving the other one and the cell-edge ratios as structural parameters to be relaxed.

In figure 1, the monoclinic mechanism is sketched as relating the initial FCC cell of the B1 phase, the intermediate $P2_1/m$ state at $\beta = 71°$, and the final CsCl-type B2 structure. The monoclinic unit-cell is obtained from the cubic $Fm\bar{3}m$ (B1) and $Pm\bar{3}m$ (B2) cells by the transformation matrices [1/2 1/2 1 / 1/2 −1/2 0 / 1/2 1/2 0] and [1 1 0 / −1 1 0 / 0 0 1], respectively, where the matrix rows contain the coefficients of linear combinations of lattice basis vectors. The second matrix also gives

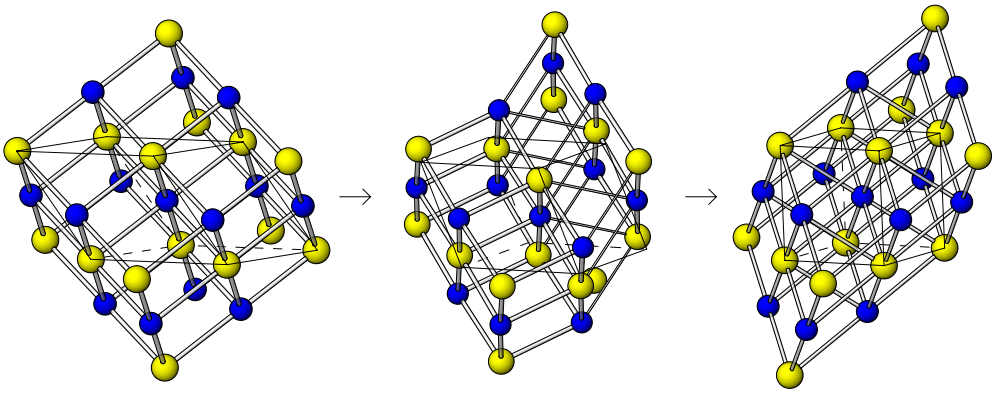

Figure 1. Structural pathway of the transformation from the B1 (left) to the B2 (right) phase with $P2_1/m$ monoclinic intermediate state (middle).

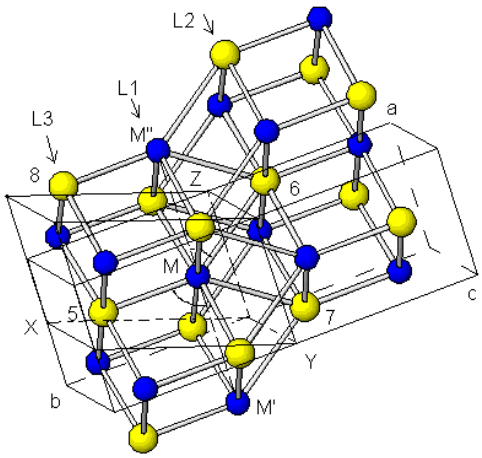

Figure 2. $P2_1/m$ intermediate state of the B1–B2 transformation at $\beta = 71°$ (cf figure 1, middle), corresponding also to the $Cmcm$ metastable phase (TlI-type structure) of NaCl. Both the orthorhombic (abc) and monoclinic (XYZ) cells are shown. The L1, L2 and L3 atomic layers with (100) monoclinic orientation, and the $\angle$Na′–Na–Cl5 and $\angle$Na″–Na–Cl6 angles are indicated.

the transformation from the primitive $Fm\bar{3}m$ cell (drawn in figure 1) to the monoclinic one. It ensues that the two cubic end phases have monoclinic cell constants $a = a_{B1}\sqrt{(3/2)}$, $b = c = a_{B1}/\sqrt{2}$, $\beta = \cos^{-1}(1/\sqrt{3}) = 54.74°$, and $a = b = a_{B2}\sqrt{2}$, $c = a_{B2}$, $\beta = 90°$, respectively. The order parameter is assumed to be $\xi = (\beta - \beta_{B1})/(\beta_{B2} - \beta_{B1}) = (\beta - \beta_{B1})/35.26°$. The monoclinic unit-cell is represented as XYZ in figure 2, where the same intermediate state sketched in the middle of figure 1 is reproduced in a different form. This particular state ($\beta = 71°$) takes the orthorhombic $Cmcm$ symmetry of the TlI-type structure, as will be discussed below, and the corresponding unit-cell (abc) is also drawn in figure 2; this is related to the monoclinic cell XYZ by the transformation matrix $[0 \quad 0 \quad 1/2 \quad 0 \quad -1/0 \quad 1 \quad 0]$. The monoclinic lattice constants are related to those of the $Cmcm$ structure according to $a = \frac{1}{2}\sqrt{(a^2_{Cmcm} + b^2_{Cmcm})}$, $b = c_{Cmcm}$, $c = a_{Cmcm}$.

A picture of the orthorhombic $Pmmn$ pathway is given in figure 3, showing again the B1 and B2 end structures with the intermediate state at $z_{Na} = 0.40$ in-between.

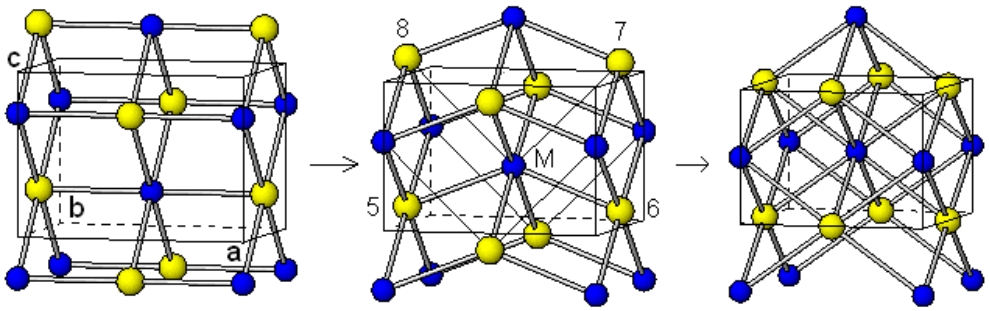

Figure 3. Structural pathway of the transformation from the B1 (left) to the B2 (right) phase with *Pmmn* orthorhombic intermediate state (middle).

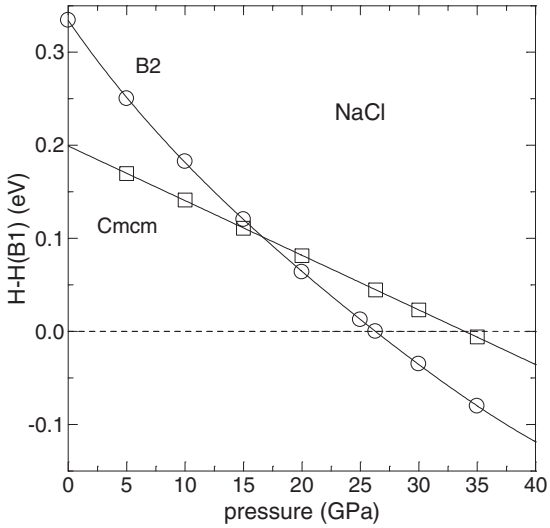

Figure 4. Enthalpies of the high-pressure B2 ($Pm\bar{3}m$, CsCl-type) and of the metastable $Cmcm$ (TlI-type) phases of NaCl, referred to that of the low-pressure B1 ($Fm\bar{3}m$, NaCl-type) phase.

The $Pmmn$ orthorhombic unit-cell is obtained from the cubic $Fm\bar{3}m$ (B1) and $Pm\bar{3}m$ (B2) cells by the transformation matrices [1 0 0 / 0 1/2 −1/2 / 0 1/2 1/2] and [1 0 1 / 1 0 −1 / 0 1 0], respectively; the two cubic end phases have orthorhombic cell constants $a = a_{B1}$, $b = c = a_{B1}/\sqrt{2}$, with $z_{Na,B1} = 1/4$, and $a = b = a_{B2}\sqrt{2}$, $c = a_{B2}$, with $z_{Na,B2} = 1/2$. The transformation coordinate is taken as $\xi = (z_{Na} - z_{Na,B1})/(z_{Na,B2} - z_{Na,B1}) = (z_{Na} - z_{Na,B1})/0.25$.

4. Results

First of all, the thermodynamic aspects of the B1–B2 phase transition of NaCl were explored by computing the enthalpies of the two end phases and of the possible intermediate one (orthorhombic $Cmcm$) versus pressure. Two internal degrees of freedom (the fractional coordinates y_{Na} and y_{Cl}) had to be relaxed in the latter case, in addition to the three unit-cell edges, for each pressure value; the x and z coordinates are fixed at 0 and 1/4, respectively. The results are plotted as differences H(B2)–H(B1) and $H(Cmcm)$–H(B1) in figure 4. From the

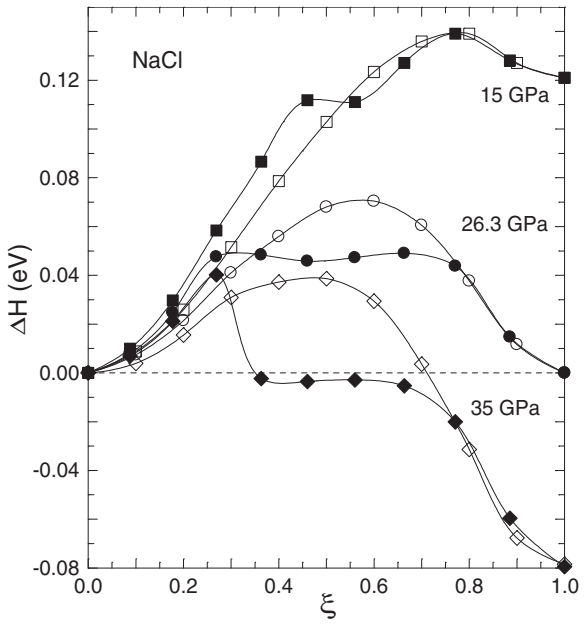

Figure 5. Enthalpy difference (per formula unit) between the intermediate state of NaCl along the B1–B2 transformation path and the B1 starting phase, as a function of the order parameter ξ, at different pressures and for two different pathways: monoclinic $P2_1/m$ (closed symbols) and orthorhombic $Pmmn$ (open symbols).

crossing points of each curve with the horizontal dashed one and with each other, the pressures of the three possible phase equilibria B1/B2, B1/$Cmcm$, and $Cmcm$/B2 are predicted to be $p_t = 26.3$, 34.0, and 16.8 GPa, respectively. However, the two latter equilibria are only virtual, as the $Cmcm$ phase appears to be never thermodynamically stable (the corresponding curve always lies above both the other ones). This confirms the experimental finding that no TlI-like orthorhombic modification of NaCl was ever observed, unlike the cases of AgCl, NaBr and NaI. The predicted B1/B2 transition pressure is only slightly lower than the experimental result of 29–30 GPa [7, 8].

The kinetic and mechanistic aspects of the B1–B2 transition were explored by calculating the $\Delta H(\xi, p)$ profiles along both the $P2_1/m$ and $Pmmn$ pathways. Nine ξ values between 0 and 1 were considered in each case, for three pressures: 15, 26.3 and 35 GPa. The six curves obtained are shown in figure 5. Quite different features appears to distinguish the monoclinic and orthorhombic mechanisms. In all curves of the second case a single intermediate maximum point is always observed, according to the normal behaviour expected for activated transition ('bottleneck') states with a simple enthalpy barrier. On the other hand, the monoclinic curves display a flat intermediate minimum at the equilibrium pressure, which turns into an inflexion point with horizontal tangent at pressures higher or lower than p_t, thus revealing the presence of a metastable phase approximately in the middle of the transformation pathway. The optimized lattice constants and atomic fractional coordinates along the transformation coordinate ξ are reported, at the equilibrium pressure only for shortness, in table 1 for the $P2_1/m$ and in table 2 for the $Pmmn$ mechanisms.

The metastable phase of the $P2_1/m$ pathway can be identified to be the TlI-like $Cmcm$ structure by considering the structural features of the intermediate state at the $\xi = 0.470$ ($\beta = 71.31°$) order parameter value of the minimum (figure 5). The monoclinic lattice becomes

Table 1. Monoclinic unit-cell constants, atomic fractional coordinates and enthalpy of the $P2_1/m$ intermediate state of NaCl, versus the B1/B2 transformation coordinate $\xi = (\beta-\beta_{B1})/(\beta_{B2}-\beta_{B1})$ at the equilibrium pressure of 26.3 GPa. The y_{Na} and y_{Cl} coordinates are fixed at 1/4.

ξ	β (deg)	a (Å)	b (Å)	c(Å)	x_{Na}	z_{Na}	x_{Cl}	z_{Cl}	ΔH (eV)
0	54.74	6.094	3.519	3.519	0.25	1	0.75	0.5	0
0.088	57.83	5.886	3.573	3.457	0.25	1	0.75	0.5	0.0079
0.177	60.99	5.687	3.627	3.406	0.2495	0.9970	0.7499	0.5034	0.0247
0.269	64.22	5.499	3.703	3.343	0.2497	0.9962	0.7499	0.5039	0.0476
0.363	67.54	5.091	3.983	3.188	0.2217	0.8767	0.7451	0.6368	0.0484
0.460	70.96	4.987	3.976	3.188	0.2210	0.8930	0.7453	0.6245	0.0458
0.560	74.48	4.889	3.989	3.179	0.2222	0.9062	0.7455	0.6126	0.0472
0.663	78.13	4.762	4.050	3.156	0.2253	0.9298	0.7464	0.5910	0.0490
0.771	81.91	4.569	4.211	3.105	0.2399	0.9800	0.7492	0.5342	0.0438
0.885	85.86	4.414	4.324	3.084	0.25	1	0.75	0.5	0.0147
1	90	4.357	4.357	3.081	0.25	1	0.75	0.5	0

Table 2. Orthorhombic unit-cell constants, atomic fractional coordinates and enthalpy of the $Pmmn$ intermediate state of NaCl, versus the B1/B2 transformation coordinate $\xi = (z_{Na} - z_{Na,B1})/(z_{Na,B2} - z_{Na,B1})$, at the equilibrium pressure of 26.3 GPa. The x_{Na}, y_{Na}, and x_{Cl}, y_{Cl} coordinates are fixed at 1/2, 1/2, and 1/2, 0, respectively.

ξ	z_{Na}	a (Å)	b (Å)	c (Å)	z_{Cl}	ΔH (eV)
0	0.250	4.976	3.519	3.519	0.75	0
0.1	0.275	4.972	3.539	3.500	0.7714	0.0074
0.2	0.300	4.958	3.588	3.457	0.7924	0.0215
0.3	0.325	4.930	3.672	3.387	0.8142	0.0410
0.4	0.350	4.883	3.764	3.318	0.8367	0.0559
0.5	0.375	4.825	3.872	3.243	0.8606	0.0680
0.6	0.400	4.749	3.979	3.184	0.8862	0.0704
0.7	0.425	4.636	4.104	3.131	0.9180	0.0605
0.8	0.450	4.493	4.239	3.098	0.9569	0.0377
0.9	0.475	4.370	4.357	3.081	0.9980	0.0116
1	0.500	4.357	4.357	3.081	1	0

orthorhombic on the condition that $c/a = 2\cos\beta$, and the $Cmcm$ symmetry is taken by the structure if $z = -x/2$ for each atom. It appears clearly that such conditions are nearly fulfilled by the structural parameters at $\beta = 70.96°$ (table 1), where $c/(2a\cos\beta) = 0.980$, $z_{Na}+x_{Na}/2 = 1.0035$, $z_{Cl}+x_{Cl}/2 = 0.9972$. By interpolation of the unit-cell edges of table 1 for $\beta = 71.31°$ one obtains $a = 4.974$, $b = 3.970$, $c = 3.188$ Å, giving $c/(2a\cos\beta) = 1.000\,06$ which satisfies completely the orthorhombic constraint. This structure is practically the same as that determined by optimization within the $Cmcm$ space group symmetry at $p = 26.3$ GPa, during the calculation of the $Cmcm$ thermodynamic curve of figure 4: $a_{Cmcm} = 3.186$, $b_{Cmcm} = 9.433$, $c_{Cmcm} = 3.976$ Å, $y_{Na} = 0.110\,35$, $y_{Cl} = 0.372\,58$, corresponding to $a = 4.978$, $b = 3.976$, $c = 3.186$ Å, $x_{Na} = 0.2207$, $z_{Na} = 0.8898$, $x_{Cl} = 0.7452$, $z_{Cl} = 0.6274$ in the monoclinic reference.

Coming back to the examination of figure 5, another difference between the $P2_1/m$ and $Pmmn$ curves is that the position of the intermediate stationary point in the former case (metastable $Cmcm$ phase) is substantially fixed half-way through the transformation, whereas the ξ value of the maximum in the latter path decreases regularly on increasing pressure. This, and other data of the enthalpy barriers, are summarized in table 3. In particular, by comparing the absolute heights of the barriers for the two different mechanisms at different pressures,

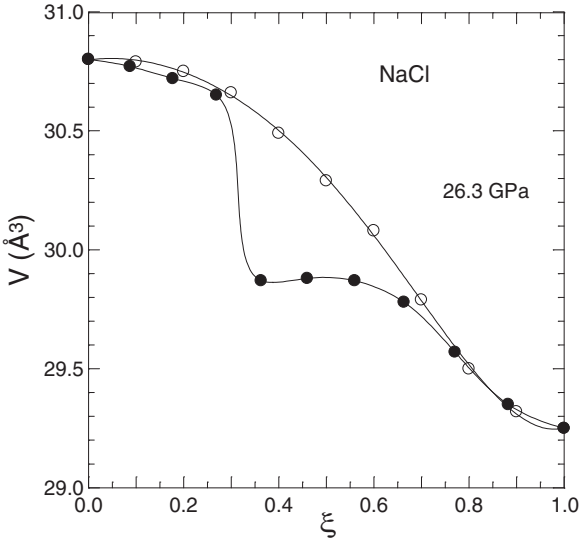

Figure 6. Volume difference (per formula unit) between the intermediate state of NaCl along the B1–B2 transformation path and the B1 starting phase, as a function of the order parameter ξ, at the equilibrium pressure. The $P2_1/m$ and $Pmmn$ pathways are denoted by closed and open symbols, respectively.

Table 3. Values of the order parameter ξ and of the enthalpy ΔH (eV), for the maxima ($P2_1/m$ and $Pmmn$ pathways) and the stationary points corresponding to the metastable $Cmcm$ phase ($P2_1/m$ pathway) in the curves of figure 5.

p	15	26.3	35 GPa
		$P2_1/m$	
ξ_{meta}	0.51	0.47	0.50
ΔH_{meta}	0.111	0.046	−0.003
ξ_{max}	0.77	0.32, 0.65	0.27
ΔH_{max}	0.139	0.048, 0.049	0.040
		$Pmmn$	
ξ_{max}	0.77	0.58	0.48
ΔH_{max}	0.139	0.070	0.039

the monoclinic pathway appears to be definitely favoured over the orthorhombic one at the equilibrium pressure (0.049 against 0.070 eV), but the situation becomes quite ambiguous at smaller and larger pressure values, where the barriers become substantially equivalent for both mechanisms. This means that, if the phase transition occurs under hysteresis (non-equilibrium) conditions, the two mechanisms may be on the same energetic grounds.

The volume behaviour of the transformation is displayed in figure 6 at the equilibrium pressure p_t. No significant qualitative changes are observed at the other two p values, and so the corresponding curves are not shown. Again the results are quite different for the two mechanisms. In the $P2_1/m$ case, a sharp volume jump is observed in the small ξ range 0.27–0.36, amounting to 50% of the total ΔV of 1.56 Å^3. Then a constant volume region follows, corresponding approximately to the metastable $Cmcm$ phase, after which V decreases smoothly to the end. On the other hand, all along the $Pmmn$ pathway the volume

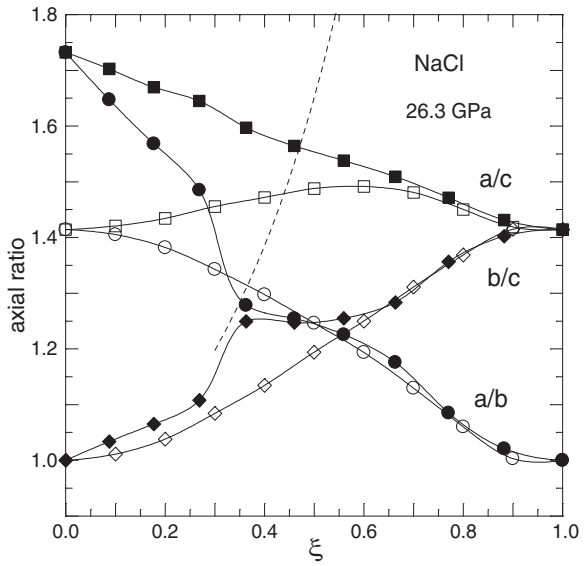

Figure 7. Unit-cell edge ratios versus the order parameter ξ along the $P2_1/m$ (closed symbols) and $Pmmn$ (open symbols) pathways. The dashed curve is the function $1/(2\cos\beta)$, which should be equal to a/c when the monoclinic unit-cell of the $P2_1/m$ mechanism acquires the $Cmcm$ symmetry of the orthorhombic metastable phase.

goes down quite continuously. It is also interesting to consider the ratios between unit-cell edges, which are plotted against the order parameter at the equilibrium pressure for the two pathways in figure 7. The most significant results are shown by a/b and b/c, which present sharp jumps exactly in the same ξ range as the volume in the $P2_1/m$ case, whereas they behave smoothly in the $Pmmn$ mechanism. The dashed curve in the same figure is the plot of the function $1/(2\cos\beta)$: when it crosses the a/c curve of $P2_1/m$ mechanism, then the monoclinic lattice becomes orthorhombic, and the $Cmcm$ metastable structure occurs; it is seen that the corresponding ξ value is the same as that of the minimum of the $P2_1/m$ enthalpy curve at 26.3 GPa (figure 5). Also the x_{Na}, z_{Na} and z_{Cl} atomic fractional coordinates of the monoclinic structure show evident discontinuities in the neighbourhood of critical ξ range 0.27–0.36 (table 1), unlike the smooth trend of z_{Cl} in the $Pmmn$ case (table 2).

5. Discussion

The most significant difference between the two transformation mechanisms considered is the discontinuous nature of the $P2_1/m$ path, at variance with the $Pmmn$ one. This is clearly reflected by the behaviour of the unit-cell constants (figures 6 and 7) and atomic coordinates. It is then interesting to investigate the atomistic basis of the monoclinic pathway in more detail. First of all, one should point out the similarities of the $P2_1/m$ intermediate state in a particular range of β values with the structure of KOH from [29]. Indeed, the unit-cell of the latter one ($a = 5.742$, $b = 3.995$, $c = 3.957$ Å, $\beta = 76.07°$) can be obtained from our monoclinic lattice by the transformation [0 0 1 / 0 1 0 / −1 0 0], so that in our reference frame it would become $a = 6.139$, $b = 3.995$, $c = 3.957$ Å, $\beta = 65.20°$, with atomic coordinates $x_{\mathrm{K}} = 0.2876$, $z_{\mathrm{K}} = 0.8842$, $x_{\mathrm{O}} = 0.7699$, $z_{\mathrm{O}} = 0.5495$. Thus, the KOH structure resembles that of the NaCl monoclinic intermediate state with $\beta \approx 65°$ ($\xi \approx 0.30$), i.e. just within the

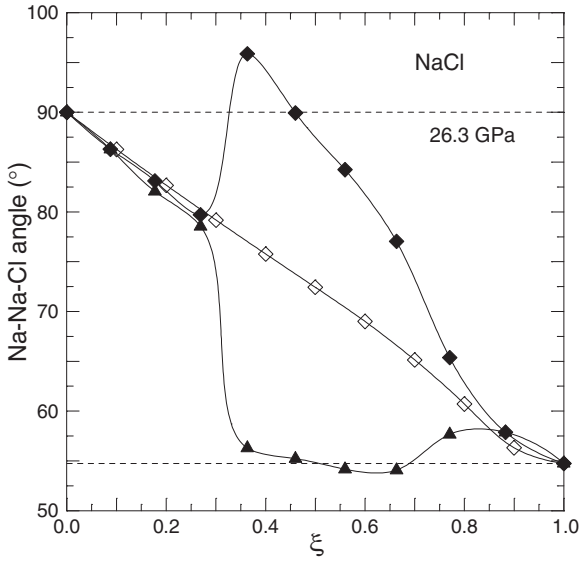

Figure 8. Angles ∠Na′–Na–Cl5 (full diamonds) and ∠Na″–Na–Cl6 (full triangles) versus the order parameter ξ along the $P2_1/m$ pathway (cf figure 2); open diamonds indicate the corresponding ∠Na–Na–Cl angle along the $Pmmn$ path.

critical ξ range where the discontinuous behaviour occurs; the only qualitative difference is due to the x_K coordinate, which approaches the complement to $1/2$ of the corresponding x_{Na} value.

Secondly, let us focus our attention on the (100) atomic layers, corresponding to (001) in the cubic B1 frame (L1, L2 and L3 in figure 2). By looking at figure 1, the first half of the transformation path can be roughly seen as a relative sliding of the adjacent L1 and L2 planes along the [001] direction ([110] in the B1 frame), whereas the L1–L3 pair does not change substantially with respect to the initial B1 configuration. Then in turn the L1 and L3 layers slide and the L1–L2 pair keep still in the second half of the pathway, so as to attain eventually the B2 structure. The relative motions inside the L1–L2 and L1–L3 plane pairs can be represented by the angles ∠Na″–Na–Cl6 and ∠Na′–Na–Cl5, respectively (figure 2), changing from 90° (B1) to 54.74° (B2) in the end structures. Such angles have been plotted versus the order parameter of the transformation in figure 8. One can see that ∠Na″–Na–Cl6 drops suddenly to approximately the final value at around $\xi = 0.315$, i.e. at the same critical value where also the discontinuities of the lattice constants are observed. A slightly more complex behaviour is shown by the other angle ∠Na′–Na–Cl5, relating the L1 and L3 layers; after a smooth initial decrease, it comes back to be right around $\xi = 0.46$, just in the neighbourhood of the $Cmcm$ intermediate structure, and then it decreases progressively down to 54.74°. Therefore, the qualitative picture of the transformation mechanism outlined above is confirmed completely, and the sharp jumps detected in the structural parameters can be explained by the adjacent L1 and L2 layers switching suddenly between the 'B1-like' (∠Na″–Na–Cl6 $\approx$ 90°) and 'B2-like' (∠Na″–Na–Cl6 $\approx$ 54.74°) configurations. The Na–Cl7 and Na–Cl8 bond distances (figure 2) behave quite similarly to the ∠Na″–Na–Cl6 and ∠Na′–Na–Cl5 angles, respectively, as is shown in figure 9. In particular, when the first angle takes the value 54.74°, then $d(\mathrm{Na}-\mathrm{Cl7}) = d(\mathrm{Na}-\mathrm{Cl6})$, so that the coordination number increases from 6 to 7 ($Cmcm$ intermediate phase), and when also the second angle becomes 54.74° then $d(\mathrm{Na}-\mathrm{Cl8}) = d(\mathrm{Na}-\mathrm{Cl5})$, attaining CN = 8 (B2 end phase).

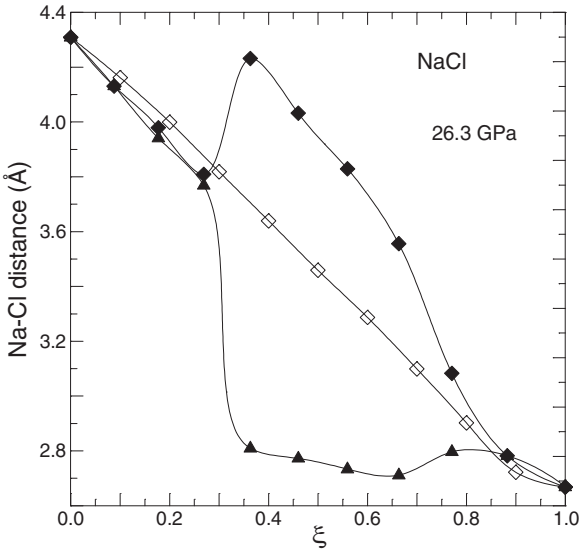

Figure 9. Na–Cl8 (full diamonds) and Na–Cl7 (full triangles) interatomic distances versus the order parameter ξ along the $P2_1/m$ pathway (cf figure 6); open diamonds indicate the corresponding Na–Cl distance along the $Pmmn$ path.

The KOH structure shows $\angle$K″–K–O6 = 66° and $\angle$K′–K–O5 = 88°, with $d(\mathrm{K}-\mathrm{O6}) = 3.164$ and $d(\mathrm{K}-\mathrm{O7}) = 3.922$ Å. It is therefore intermediate between the B1 and $Cmcm$ structures, and is stabilized by the need for hosting the H atom (bonded to O7) approximately along the K–O7 direction. Actually, here the L1 to L2 inter-layer distance is expanded by 7.3% with respect to the L1–L3 value, against a corresponding contraction of 4% in the NaCl intermediate state with comparable β angle. This effect is related to the different values of the x_{K} and x_{Na} relaxed coordinates, as discussed above: in the KOH case all H atoms are located in the L1–L2 but not in the Li–L3 inter-layer region, so as to force the former one to expand. In the $P2_1/m$ intermediate state of NaCl, on the other hand, at high pressure the L1–L2 inter-layer region is more easily compressible because of the misfit between the two atomic planes.

As for the $Pmmn$ mechanism, it is clear that the L2 and L3 (100) atomic layers (figure 3) are constrained by the mirror plane to slide together with respect to L1, as the order parameter goes from 0 to 1. The corresponding $\angle$Na–Na–Cl angle decreases smoothly and nearly linearly from 90° to 54.74° as ξ increases (figure 8). A similar continuous trend is shown by the inter-layer Na–Cl bond distance (figure 9). Clearly, in this case the symmetry constraint prevents a two-step mechanism with different sliding of adjacent atomic planes, as in the $P2_1/m$ mechanism.

6. Conclusions

A detailed quantum-mechanical calculation of the enthalpic and structural changes versus the transformation coordinate at constant pressure has allowed us to compare the monoclinic $P2_1/m$ and orthorhombic $Pmmn$ pathways of the rocksalt to CsCl-like phase transition of NaCl. It has been found that, at the equilibrium pressure p_{t}, the former mechanism is definitely favoured energetically, similarly to what previously predicted for CaO; however, both positive

and negative deviations of the pressure from p_t tend to equalize the enthalpy barriers of the two pathways, indicating that hysteresis phenomena may substantially influence the activation balance between different kinetic mechanisms. While the $Pmmn$ transformation can be seen as a continuous slide of all adjacent atomic planes, in the $P2_1/m$ case the process occurs basically in two steps, where every second plane moves and adjacent pairs keep their relative positions. This accounts for the discontinuous character of the monoclinic mechanism as revealed by the calculations, and for the formation of the metastable intermediate $Cmcm$ phase along the corresponding pathway. A still open question, to be clarified in future work, concerns the different behaviour of other sodium and silver halides, where the TlI-like and/or the KOH-like phases present stability fields of their own at high pressure, at variance with the NaCl and CaO cases.

References

[1] Toledano J C and Toledano P 1987 *The Landau Theory of Phase Transitions* (Singapore: World Scientific)
[2] Toledano P and Dmitriev V 1996 *Reconstructive Phase Transitions* (Singapore: World Scientific)
[3] Catti M 2001 *Phys. Rev. Lett.* **87** 035504
[4] Catti M 2002 *Phys. Rev.* B **65** 224115
[5] Tonkov E Yu 1992 *High Pressure Phase Transformations, a Handbook* (London: Gordon and Breach)
[6] Yagi T, Suzuki T and Akimoto S 1983 *J. Phys. Chem. Solids* **44** 135
[7] Bassett W A, Takahashi T, Mao H K and Bell P M 1968 *J. Appl. Phys.* **39** 319
[8] Heinz D L and Jeanloz R 1984 *Phys. Rev.* B **30** 6045
[9] Léger J M, Haines J, Danneels C and de Oliveira L S 1998 *J. Phys.: Condens. Matter* **10** 4201
[10] Kusaba K, Syono Y, Kikegawa T and Shimomura O 1995 *J. Phys. Chem. Solids* **56** 751
[11] Hull S and Keen D A 1999 *Phys. Rev.* B **59** 750
[12] Jochym P T and Parlinski K 2001 *Phys. Rev.* B **65** 024106
[13] Richet P, Mao H K and Bell P M 1986 *J. Geophys. Res.* **93** 15279
[14] Sato Y and Jeanloz R 1981 *J. Geophys. Res.* **86** 1773
[15] Liu L G and Basset W A 1972 *J. Geophys. Res.* **77** 4934
[16] Froyen S and Cohen M L 1986 *J. Phys. C: Solid State Phys.* **19** 2623
[17] Martín Pendás A, Luaña V, Recio J M, Florez M, Francisco E, Blanco M A and Kantorovich L N 1994 *Phys. Rev.* B **49** 3066
[18] Sims C E, Barrera G D, Allan N L and Mackrodt W C 1998 *Phys. Rev.* B **57** 11164
[19] Habas M P, Dovesi R and Lichanot A 1998 *J. Phys.: Condens. Matter* **10** 6897
[20] Buerger M 1948 *Phase Transformations in Solids* ed R Smoluchowski, J E Mayers and W A Weyl (New York: Wiley) p 183
[21] Watanabe M, Tokonami M and Morimoto N 1977 *Acta Crystallogr.* A **33** 284
[22] Okai B 1980 *J. Phys. Soc. Japan* **48** 514
[23] Onodera A, Kawano S, Nakai Y and Achiwa N 1992 *Physica* B **180/181** 279
[24] Stokes H T and Hatch D M 2002 *Phys. Rev.* B **65** 144114
[25] Catti M 2003 *Phys. Rev.* B **68** 100101(R)
[26] Saunders V R, Dovesi R, Roetti C, Orlando R, Zicovich-Wilson C M, Harrison N M, Doll K, Civalleri B, Bush I J, D'Arco Ph and Llunell M 2003 *CRYSTAL03: User's Manual* University of Torino, Italy, and CLRC Daresbury Laboratory, UK
[27] Perdew J P, Burke K and Ernzerhof M 1996 *Phys. Rev. Lett.* **77** 3865
[28] Prencipe M, Zupan A, Dovesi R, Aprà E and Saunders V R 1995 *Phys. Rev.* B **51** 3391
[29] Jacobs H, Kockelkorn J and Tacke T 1985 *Z. Anorg. Allg. Chem.* **531** 119